Future Journal of Pharmaceutical Sciences

RESEARCH Open Access

Development of trigger sensitive hyaluronic acid/palm oil-based organogel for in vitro release of HIV/AIDS microbicides using artificial neural networks

M. O. Ilomuanya[1*], R. F. Elesho[1,2], A. N. Amenaghawon[3], A. O. Adetuyi[1], Vijayalakshimi Velusamy[4] and A. S. Akanmu[5]

Abstract

Background: Efficient and effective chemotherapeutic methods designed to prevent the continuous spread of HIV/AIDS is essential to break the cycle of new infections. The use of condoms has been seen to be effective in prevention of HIV and STIs but its lack of use especially in vulnerable population is a deterrent to its overall success as a control method. Utilization of topical microbicide to curb the spread of HIV follows the current paradigm for HIV prevention in at risk individuals. The objective of this study was to develop and evaluate hyaluronic acid/palm oil-based organogel loaded with maraviroc (MRV) which would be released using hyaluronidase as the trigger for pre-exposure prophylaxis of HIV.

Results: The organogels had average globules size 581.8 ± 3.9 nm, and were stable after three freeze thaw cycles; the thermosensitive and HA sensitivity was achieved via incorporation of hyaluronic acid and dicaprylate esters in the organogel with thermogelation occurring at 34.1 °C. Artificial neural network was used to model and optimize mucin absorption and flux. These responses were predicted using the multilayer full feed forward (MFFF) and the multilayer normal feed forward (MNFF) neural networks. Optimized organogel showed the mucin adsorption and flux was 70.84% and 4.962 μg/cm^2/min$^{1/2}$, hence MRV was adequately released via triggers of temperature and HA. The MRV organogel showed inhibition HIV − 1 via TZM-bl indicator cells. Compared to control HeLa cells without any treatment, MRV organogel was not cytotoxic for 14 days in vitro.

Conclusion: These data highlight the potential use of hyaluronic acid/palm oil-based organogel for vaginal delivery of anti-HIV microbicides. This can serve as a template for more studies on such formulations in the area of HIV prevention.

Keywords: HIV prophylaxis, Maraviroc, Organogel, Artificial neural networks

Background

Utilization of more potent antiviral agents in novel formulation that target the virus at critical steps in its replication cycles are pertinent in the discovery of the ideal HIV microbicide [1]. These potent antiviral agents require a drug carrier that meets the requirements for vaginal delivery which include cervicovaginal tissue safety and ease of application by clients [2, 3]. Organogels which are gel-based delivery systems act by immobilization of apolar solvents due to formation of three-dimensional aggregates via fluid filled mechanisms which possess intrinsic thermodynamic stability. They do not demonstrate wetness and have increased vaginal retention on application [4]. The current paradigm for topical microbicide development has been focused on antiretroviral drugs as earlier work evaluating non-specific entry inhibitors showed no benefit to the participants in those clinical trials [5]. Maraviroc, a CCR5 antagonist, selectively and reversibly binds to the chemokine coreceptors located on human CD4 cells. CCR5 antagonism prevents interaction between the human CCR5 coreceptor and the

* Correspondence: milomuanya@unilag.edu.ng; milomuanya@live.com
[1]Department of Pharmaceutics and Pharmaceutical Technology, Faculty of Pharmacy, University of Lagos, PMB 12003, Surulere, Lagos, Nigeria
Full list of author information is available at the end of the article

gp120 subunit of the viral envelope glycoprotein, causing gp 120 conformational change disruption. This prevents CCR5-tropic HIV-1 fusion with the CD4 cell hence inhibiting cell entry [6]. Utilization of a novel delivery form which is muco/bio-adhesive and ensures drug release due to predetermined trigger will be a useful approach in ensuring utilization and delivery of maraviroc as a microbicide for vaginal application [5, 7].

Hyaluronic acid has been used owing to its biodegradable, non-immunogenic, and bio-adhesive properties [8, 9]. It is a non-sulfated, hydrophilic, naturally occurring anionic muco-polysaccharide made of repeating disaccharide units of D-glucuronic acid and *N*-acetyl-D-glucosamine, linked through β(1–4) and β(1–3) glycoside bonds [10, 11]. Hyaluronic acid (HA) is hydrolysable under treatment with the hyaluronidase enzyme, which is abundant in human seminal fluid [10] as well as other body fluids and tissues [10, 11].

Palm oil is an edible vegetable oil derived from the mesocarp of the fruit of the oil palms, primarily the African oil palm *Elaeis guineensis*, and to a lesser extent from the American oil palm *Elaeis oleifera* and the maripa palm *Attalea maripa* [12]. Phytonutrients in palm oil beneficial to pharmaceutical products are vitamin E, carotenes, and triglycerides. The concentration of vitamin E (tocotrienol and tocopherol) and carotenes were found to be higher compared to other natural oils such as corn and olive oil [13, 14]. Lipid-based formulations containing palm oil have been used in formulation of creams and gels due to its excellent safety profile. Palm oil-based formulations are unaffected by excipients such as hyaluronic acid when mixed in a formulation, but rather the drug performance and stability were enhanced during delivery [12, 14].

Inspired by biological neural network, artificial neural networks (ANN) could build up the mathematical relationship between the input parameters and the output parameters, with the advantage that it can be modeled without prior knowledge. An ANN facilitates the ability to learn complex nonlinear relationships between input and output parameters [15]. For the current work, artificial neural networks are used to model and optimize mucin absorption and flux. These responses were predicted using the multilayer full feed forward (MFFF) and the multilayer normal feed forward (MNFF) neural networks. In this proposed study, bio-adhesive properties imparted on this formulation will be leveraged upon to impart the 'smart' organogel feature of trigger release of maraviroc from the hyaluronic acid/palm oil (HAP)-based organogel drug carrier for pre-exposure prophylaxis of HIV.

Methods

Materials

Refined palm oil (Raffles oil LFTZ Enterprise Lagos) Labrafac Lipophile WL 1349 (Batch 172,945 Gattefosse SAS); trifluoro acetic acid (Lot#M56718067 Shanghai Macklin Biochemical Co., Ltd.); hyaluronic acid sodium salt (Shanghai Macklin Biochemical Co., Ltd.); hyaluronidase (HAase) from bovine testes with a specified activity of 810 U/mg, bovine serum albumin (BSA, Fraction V); mucin from porcine stomach (CAS: 84082-64-4 Shanghai D&B Biological Science and Technology Co. Ltd.); Maraviroc (Cat# 11580, Lot# 15057WB-67 Fisher Bioservices/NIH-ARP German town MD); Nonoxylol (Sublot code 946 DPT Laboratories Ltd., San Antonio, TX 78215 USA); periodic acid (CAS No. 10450-60-9 Loba Chemie Pvt. Ltd.); Cremophor EL CAS:61791-12-6 (Shanghai Macklin Biochemical Co., Ltd). Dialysis membrane (molecular weight cut off: 12–13 kDa, white gridded, MERCK). All other chemicals were of analytical grades and used as obtained from suppliers.

Design of experiment

For the current study, a three-factor central composite design (CCD) was used to develop the experimental design to study the response pattern and to determine the optimum combination of variables for maximizing the chosen responses. The CCD combines the vertices of a hypercube whose coordinates are given by a 2^n factorial design with star points. The star points provide the estimation of curvature of the nonlinear response surface. Table 1 shows the range and levels of variables optimized. The experimental runs were performed in a random manner in order to minimize the effects of unexplained variability in the response [16]. The independent variables investigated were HA Concentration, volume of surfactant, and reaction time. The responses or dependent variables investigated were mucin adsorption (%) and flux (μg/cm^2/min$^{1/2}$). The values of the independent variables were calculated using Eq. (1). The experimental design was developed using the data in Table 1 with Design Expert® software version 7.0.0 (Stat-ease, Inc. Minneapolis, USA). The values of the independent variables were calculated using Eq. (1).

$$x_i = \frac{X_i - X_o}{\Delta X_i} \tag{1}$$

where x_i and X_i are the coded and actual values of the independent variable respectively. X_o is the actual value

Table 1 Coded and actual levels of the factors for three factor central composite

Independent variables	Symbols	Coded and actual levels				
		− 1.68	− 1	0	1	1.68
HA concentration	X_1	0.10	0.12	0.15	0.18	0.20
Volume of surfactant	X_2	4.90	5.22	5.70	6.18	6.50
Reaction time	X_3	0.20	0.26	0.35	0.44	0.50

of the independent variable at the center point, and ΔX_i is the step change in X_i.

Artificial neural network modeling

For the current work, commercial ANN Software, Neural Power, version 2.5 (C.P.C-X Software USA) was used to model and optimize Mucin adsorption and flux. These responses were predicted using the MFFF and the MNFF neural networks. These networks were trained using different learning algorithms such as incremental back propagation (IBP), batch back propagation (BBP), quick propagation (QP), generic algorithm (GA), and Levenberg-Marquadt algorithm (LM). The ANN architecture was made up of an input layer, a hidden layer, and an output layer. The optimal network topology was determined using only one hidden layer, while the number of neurons in this layer and the transfer function of the input and output layer were determined iteratively by developing several neural networks with different transfer functions (Sigmoid, Hyperbolic-tangent, Gaussian, Linear, Threshold, Linear, and Bipolar Linear). Each of the network was trained using a stopping criterion of 100,000 iterations [17]. The learning algorithms employed 70% of the experimental data as training set, 15% as validating set, and the remaining 15% as testing set. This was to evaluate the predictive ability of the model with respect to the hidden data which were not used for training and to appraise the generalization capacity of the ANN [18, 19].

ANN data validation

The efficiency of the developed ANN models in its prediction capability of the responses (Flux and mucin adsorption) was evaluated extensively for the process. Statistical indicators which include coefficient of determination (R^2), root mean square error (RMSE), mean absolute deviation (MAD), and average absolute deviation (AAD) were employed for this purpose. These terms are defined by Eqs. (2, 3, 4, 5, and 6) [17].

$$R^2 = 1 - \sum_{i=1}^{n} \left(\frac{\left(y_{\exp} - y_{pred}\right)^2}{\left(y_{\exp} - y_{\exp,ave}\right)^2} \right) \tag{2}$$

$$\text{Adjusted } R^2 = 1 - \left[\left(1 - R^2\right) \times \frac{n-1}{n-k-1} \right] \tag{3}$$

$$\text{RMSE} = \left(\frac{1}{n} \sum_{i=1}^{n} \left(y_{pred} - y_{exp}\right)^2 \right)^{1/2} \tag{4}$$

$$\text{AAD}(\%) = \left(\frac{1}{n} \sum_{i=1}^{n} \left(\frac{y_{\exp} - y_{pred}}{y_{\exp}} \right) \right) \times 100 \tag{5}$$

$$\text{MAD} = \frac{1}{n} \sum_{i=1}^{n} \left| y_{pred} - y_{pred,avg} \right| \tag{6}$$

Where n is the number of points

K is the number of input variables
y_{pred} is the predicted value obtained from the model
$y_{\exp}$ is the actual value
$y_{\text{ave, exp}}$ is the average of the actual values.

The coefficient of determination (R^2) gives an indication of consistency between the experimental values and predicted value. The closer the R^2 value is to 1, the better the model fits to the actual data. The value of R^2 should be at least 0.8 for a good fit of a model [19, 20]. R^2 is a measure of the amount of the reduction in the variability of the response by using the repressor variables in the model while RMSE and AAD are direct methods for describing deviations. The RMSE, AAD, and MAD between predicted and experimental values must be as small as possible [16].

Optimization of responses

The optimum values of the responses were obtained by algorithm-based optimization. The optimization process searches for a combination of factor levels that simultaneously satisfy the criteria placed on each of the responses and factors. To include a response in the optimization criteria, it must have a model fit through analysis or supplied via an equation only simulation. For this work, the optimization was done by maximizing the desired responses. The optimization algorithms considered were genetic algorithm, particle swarm optimization, and rotation inherit optimization.

Preparation of organogels

Surfactant mixtures of polyoxyethylene sorbitan monooleate and Labrafac® (Propylene glycol Dicarprylate) were prepared. Specified amount of the surfactant mixtures (as shown in Table 3) was added to 2.45 ml refined palm oil containing 0.1% w/w maraviroc in beaker and kept on magnetic stirrer. The above mixture was stirred on a magnetic stirrer at 80 rpm using varying time intervals (as shown in Table 3). Subsequently, 1 ml double-distilled water containing a specified amount of dispersed hyaluronic acid (Table 3) was added dropwise to the surfactant-oil solution with the use of a micropipette. Additional water to make up to 10 ml was introduced until the formation of the organogel was achieved. Based on the composition of the surfactant-oil-water mixture, the systems either formed gelled structures, emulsion, or remained as a liquid mixture. A ternary phase diagram was plotted to find the area of the gelation using Origin 8 (Professional) software. The

organogels were observed for their color, odor, appearance, and texture. The microstructure of the organogels were analyzed under bright Binocular Camera Microscope. The organogels prepared with aqueous rhodamine B solution were visually examined to understand the phenomenon of the gelation. The photographs of the samples were taken with a 10-megapixel Canon DSLR camera.

Physicochemical testing

Rheological profile was determined using the CP52 spindle on a cone/plate Brook field Model HADVIII+ viscometer (Brookfield Eng. Lab., Inc., Middlebrow, MA). Data was collected using Rheocalc software (Brook field Eng. Lab., Inc.). pH and osmolality measurements were taken using Mettler Toledo S975 Multiparameter Meter with Stirrer and Probes for pH, osmolality.

Accelerated thermal stability studies

Thermocycling method of accelerated stability test was used to analyze the long-term stability of the organogels. Freshly prepared samples were subjected alternatively at 80 °C for 15 min in a water bath and subsequently at − 20 °C temperature-controlled cabinet for the next 15 min. This constituted 1 cycle. The experiment was continued for 4 cycles. The samples were continuously monitored for any signs of destabilization. The organogels were regarded as destabilized if there was a phase separation. Organogels were also regarded as destabilized if they failed to maintain their structural integrity. The samples were regarded as stable, if they were able to sustain three cycles of thermocycling without any signs of destabilization.

Thermal analysis

The gel to sol transition (T_{GS} °C) of the organogels was determined by falling ball method. Two grams of the organogels was poured in a 10 ml test tube. A stainless steel ball (diameter: 1/8th of an inch; weight = 130 mg) was placed gently on the top of the organogels. The test tube was heated at a rate of 1 °C/min in a melting point determination apparatus. The temperature at which the stainless steel ball started to move into the gel was noted as the T_{GS} °C of the organogels.

Fourier transform infrared spectroscopy

The interactions among the components of organogels were analyzed by Fourier-transform infrared (FTIR) spectroscopy using alpha-E, Bruker, Germany. The analysis was conducted in attenuated total reflectance (ATR) mode.

X-ray diffraction analysis

The organogels were analyzed by X-ray diffractometer using Cu-Kα radiation generated at 30 kV and 20 mA. The scanning range was 5° to 50° 20 at a step size of 2°/min.

Mucoadhesion study

Mucin adsorption was evaluated utilizing periodic acid and Schiffs colorimetry. Mucin was dissolved in simulated seminal fluid and mixed in a 1:1 ratio of the maraviroc containing HAP organogel formulation containing varying concentrations of hyaluronic acid (Table 3). The suspension was under 100 rpm agitation in a water bath shaker at 37 °C for 40 min. Centrifugation at 400 rpm for 120 s was carried out prior to supernatant recovery. To 1 ml of supernatant, 0.2 ml of periodic acid reagent was added and incubated at 37 °C for 2 h, followed by the addition of 0.2 ml Schiff reagent and incubation at 25 °C for 30 min. The absorbance was recorded at 555 nm. The mucin content was calculated from the standard calibration curve and plain organogel without hyaluronic acid was utilized as control. Each experiment is performed in triplicate with mucin adsorption calculated using Eq. 7

$$\%\text{Mucin adsorption} = \left(\text{total mass of mucin} - \text{free mucin total mass of mucin}\right) \times 100 \tag{7}$$

In vitro drug release analysis of HA-palm oil-based organogel

The in vitro drug release studies were carried out using a modified Franz's diffusion cells. Dialysis membrane was used to separate the donor and the receptor chamber. Accurately weighed samples (1 g) were loaded in the donor compartment and placed gently into the receptor compartment so that the dialysis membrane was in contact with the receptor fluid. Twenty-five milliliters of 1% Cremophor EL in double-distilled water was used as the dissolution medium and was kept stirring at 100 rpm and the temperature was maintained at 37 ± 1 °C. Samples were taken from the receptor compartment at predetermined time intervals (5, 10,15, 30 min) and assayed for drug content using a high-pressure liquid chromatography method. Separations were done by gradient elution. The initial step used 70% (v/v) of 0.1% TFA in water and 30% (v/v) of 0.05% TFA in acetonitrile; the wavelength for the detection of maraviroc (MRV) was 210 nm.

Enzyme degradation analysis of HAP organogel utilizing hyaluronidase

Bovine testicular hyaluronidase (HYase) was utilized in this study as it facilitates hydrolytic decomposition of β 1-4 glycosidic bonds situated in hyaluronic acid utilized

in formulation of the organogel. Twenty milligrams of the organogel was dispersed in 3 ml of a mixture of freshly formulated simulated vaginal fluid and simulated seminal fluid in the ration of 1:4 (this simulates the volumes encountered during ejaculatory intercourse). The pH was adjusted to 7.1 to simulate ejaculatory intercourse pH conditions. The organogel and simulant mixture was introduced into a test tube shaker bath at 37 °C ± 0.5 °C and aliquot volumes of 400 μl was obtained at 0.5, 1, 6, 12, 24, 36, 48, 72, 96 h. The aliquot volumes were then heated at 100 °C ± 1.1 °C to inactivate HYase, and glucuronic acid was released as measured using UV-Vis spectrophotometry at 530 nm. Percentage cumulative release of maraviroc was also calculated in the presence and absence of HYase.

Safety testing

Lactobacillus crispatus viability assay

L. crispatus ATCC33197 were obtained from the American Type Culture Collection (VA, USA). Bacterial suspensions were prepared by selecting isolated colonies from fresh, overnight culture plates and suspending the test organisms in saline to a density of a 2 McFarland standard. Suspension were mixed 1:1 with each gel. After incubation at 35 °C for 30 min, samples were plated onto the appropriate medium. Plates were incubated for 24 h and evaluated for killing of the test microorganisms by examination. Colony forming units were counted and the difference between the untreated and treated cultures were determined. The percentage of *L. crispatus* viability was calculated and plotted.

Efficacy testing

TZMB assay

The TZM-bl cells were seeded in 24-well plates to obtain an optical density corresponding to 2×10^5 cells in each well. After 24 h, the cells were treated with dilutions of the formulations optimized HAP organogel containing Maraviroc, HAP organogel containing Maraviroc (F5), and nonoxynol-9 gel. After 24 h, the media from all wells was suctioned out to remove the dilutions of formulation and replaced with fresh media. This was followed by the cells were inoculated with 25 μl HIV-1 NL4-3 virus for 3 h. After 24-h incubation, the cells were washed with phosphate-buffered saline, lysed with 150 μl Mammalian Protein Extraction Reagent, centrifuged, and the lysate treated with luciferase after which the lysate is obtained after centrifugation is treated with luciferase. Luminesce was measured using a luminometer (Promega WI, USA). The results of the treatment were compared with control (HIV-infected cells without antiretroviral treatment) and data obtained was plotted to obtain an HIV infectivity dose-response. All the experiments were performed in triplicate.

In vitro cytotoxicity studies

Long-term in vitro cytotoxicity of optimized HAP organogel, HAP organogel (F5), and nonoxynol 9 was evaluated in HeLa cells. Briefly, cells were seeded in 12-well plates at a density of 1.0×10^4 cells/well in triplicate and allowed to attach to wells overnight. HAP organogel were added to obtain an MRV concentration of 5 μg/ml in each well. Blank gel containing no drug (50 μl) was added to triplicate wells to determine cytotoxicity of this component. Cell viability was assessed on days 1, 2, 4, 7, 10, and 14 as per MTT method [5]. The absorbance obtained for MRV was compared to control cells (no treatment). Assuming non-Gaussian distribution, nonparametric statistics were used to determine significance.

Results

Modeling and analysis using artificial neural network

Two networks architectures were considered and trained using different training algorithms to determine the one most suitable for the intended purpose. The best training algorithm was the Levenberg-Marquadt (LM) algorithm (Table 2) and while the best network architecture was a MFFF network. This was chosen because network architecture and training algorithm are characterized by low RMSE and high R^2 values. To determine the optimum network topology, iterations were also carried out on the various transfer functions. The best transfer function was also used to determine the optimum number of neurons for the network. The Hyperbolic-Tangent function gave higher R^2 values compared all other transfer functions.

Optimum number of neurons

In order to determine the optimum number of neurons in the hidden layer, iterations were carried out with the hyperbolic tangent transfer function. From Fig. 1a, the

Table 2 R^2 and RMSE values of MNFF and MFFF using different training algorithms

Network architecture	Training algorithm	Response			
		Mucin adsorption		Flux	
		RMSE	R^2	RMSE	R^2
MNFF	IBP	7.34217	0.76591	0.19291	0.91433
	BBP	15.81500	− 0.0859	0.21300	0.89556
	QP	13.71700	0.18308	0.59388	0.18807
	GA	7.57710	0.75073	0.22576	0.88267
	LM	6.83070	0.79741	0.24737	0.85912
MFFF	IBP	6.56520	0.81286	0.12781	0.9624
	BBP	16.91100	− 0.24175	0.69043	− 0.09741
	QP	14.09100	0.13784	0.59431	0.18689
	GA	7.92070	0.72760	0.29926	0.79383
	LM	6.55470	0.81435	0.12148	0.96603

A

No of neurons	Mucin adsorption	Flux
1	0.69563	0.31349
2	0.78527	0.15893
3*	**0.81345**	**0.96603**
4	0.81345	0.96603
5	0.81345	0.96603
6	0.81345	0.96603
7	0.81345	0.96603

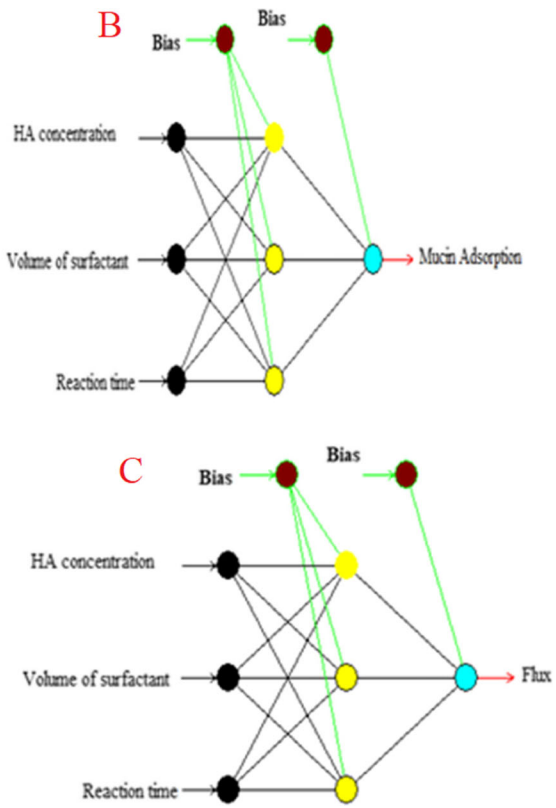

Fig. 1 **a** Determination of optimum number of neurons. **b** Architecture of the optimal ANN for predicting mucin adsorption. **c** Architecture of the optimal ANN for predicting flux

optimum number of neurons in the hidden layer is 3. This was chosen as the number of neurons that yielded the highest R^2 value. The optimum network topology thus becomes 3-3-1 for each response, i.e., three input factors in the input layer, three neurons in the hidden layer, one response in the output layer, and a hyperbolic tangent transfer function for the hidden and output layers (Fig. 1b, c). The optimum ANN topology has adequately high R^2 (0.96603) value for the prediction of flux and a sufficiently high R^2 for prediction of Mucin adsorption. These values obtained implies that the ANN model can be used to predict these responses from the input factors.

Validation of ANN model results

The values of mucin adsorption and flux as predicted by the optimum network topology are presented in Table 3 alongside the experimental values for comparison. Comparison of the actual experimental values of the response and those predicted by the ANN model show that there was a reasonable agreement. This implies that the deviation of the predicted values from the actual was minimal. The closeness of the experimental and predicted values of the responses shows the validity of the ANN model.

Mucin adsorption deviation for run 10, 16, and 19 had increased variation compared to other runs due to experimental variation; however, the goodness of fit statistics of the models for mucin adsorption indicate a good fit between the experimental results and the results predicted by the model when looking at the entire data set in its totality (Table 4). The goodness of fit statistics of the models for mucin adsorption and flux are shown in Table 4. The values obtained indicate a good fit between the experimental results and the results predicted by the model. This is corroborated by the high value of R^2 and adjusted R^2 values with the error terms (RMSE, AAD, MAD) being relatively small compared to the mean of the observations.

Response surface plots, optimization of input factors, and responses

The response surface plots presented in Fig. 2a–d show the relationship between the responses (mucin adsorption and flux) and the input factors (HA concentration, volume of surfactant, reaction time). The optimization of the input factors and the response was carried out using genetic algorithm (GA), particle swarm optimization (PSO), and rotation inherit optimization (RIO) and the results are summarized in Tables 5 and 6.

Table 3 Comparison of experimental results with ANN predicted results

Run	Factors			Responses			
				Mucin adsorption (%)		Flux (μg/cm^2/min$^{1/2}$)	
	HA concentration (ml)	Volume of surfactant (ml)	Reaction time (min)	Experiment	Predicted	Experiment	Predicted
1	0.12	5.22	0.26	23.11	23.11	3.85	3.85
2	0.12	6.18	0.26	21.23	21.23	2.99	2.99
3	0.12	6.18	0.44	39.72	39.72	3.73	3.73
4	0.15	6.50	0.35	55.73	55.73	4.11	4.11
5	0.15	5.70	0.50	68.73	68.73	4.83	4.83
6	0.18	5.22	0.26	21.45	21.45	2.78	2.78
7	0.12	5.22	0.44	37.50	37.50	3.98	3.98
8	0.18	5.22	0.44	28.33	28.33	2.97	2.97
9	0.18	6.18	0.44	31.98	31.98	3.09	3.09
10	0.15	5.70	0.35	32.99	50.84	4.01	4.06
11	0.20	5.70	0.35	33.87	33.87	3.11	3.11
12	0.15	5.70	0.35	59.99	50.84	4.21	4.06
13	0.15	5.70	0.20	46.77	46.77	4.11	4.11
14	0.10	5.70	0.35	25.78	25.78	2.67	2.67
15	0.18	6.18	0.26	23.01	23.01	2.33	2.33
16	0.15	5.70	0.35	35.88	50.84	3.63	4.06
17	0.15	4.90	0.35	44.67	44.67	3.42	3.42
18	0.15	5.70	0.35	57.32	50.84	4.32	4.06
19	0.15	5.70	0.35	60.11	50.84	4.11	4.06
20	0.15	5.70	0.35	58.73	50.84	4.08	4.06

From the results, it can be seen that the values obtained from the three optimization methods were approximately equivalent.

Physicochemical characterization of the optimized HAP, HAP organogel (F5)

Utilizing a reaction time of 0.5 min, hyaluronic acid concentration of 0.148 ml, and volume of surfactant 6.19 ml, 0.1% w/w maraviroc uniformly dispersed in the oil-phased formed optimized HAP organogel with an agreeable odor. A reaction time of 0.5 min, hyaluronic acid concentration of 0.15 ml, and volume of surfactant 5.7 ml, 0.1%w/w maraviroc uniformly dispersed in the oil phased-formed HAP organogel, a slightly yellow gel (see run 5 in Table 3). The optimized gel was off white having a pH of 4.9 and an osmolality of 299 mOsm/kg. These values differ slightly from the pre optimized gel analyzed which had a slightly yellow color and pH of 5.9 and an osmolality of 320.4 mOsm/kg. The viscosity of the organogels decreased as an increased shear was applied to them thus mimicking a pseudoplastic system. All the gels formulated had comparable viscosities as shown Table 7. The X-ray diffraction (XRD) profile of organogel showed a broad hump at approximately 20 °C 2Θ showing the predominant amorphous nature of the organogel (Fig. 3a). The presence of aggregated granular structures leads to the formation of a three-dimensional network structure. With the increase in the concentration of surfactant mixture, there was a corresponding increase in the three-dimensional networked structure as visualized under the microscope (Fig. 3 d–f). FTIR spectra of the formulation showed a broad peak at 3410 cm^{-1} attributed to the presence of maraviroc and appearing peaks of 2911 and 2849 cm^{-1} attributed C-H functional groups (Fig. 3b).

Nonoxynol-9 is chosen as a placebo for comparison with the formulated organogels because it is the most commonly used spermicide in the world with a favorable safety profile. It has no activity against HIV [21]. The

Table 4 Goodness of fit statistics for ANN models

Parameter	Response	
	Mucin adsorption	Flux
R^2	0.81345	0.96603
Adj R^2	0.77848	0.95966
Mean	40.3451	3.6165
RMSE	6.3887	0.1184
AAD	7.5609	1.1823
MAD	11.7471	0.5572

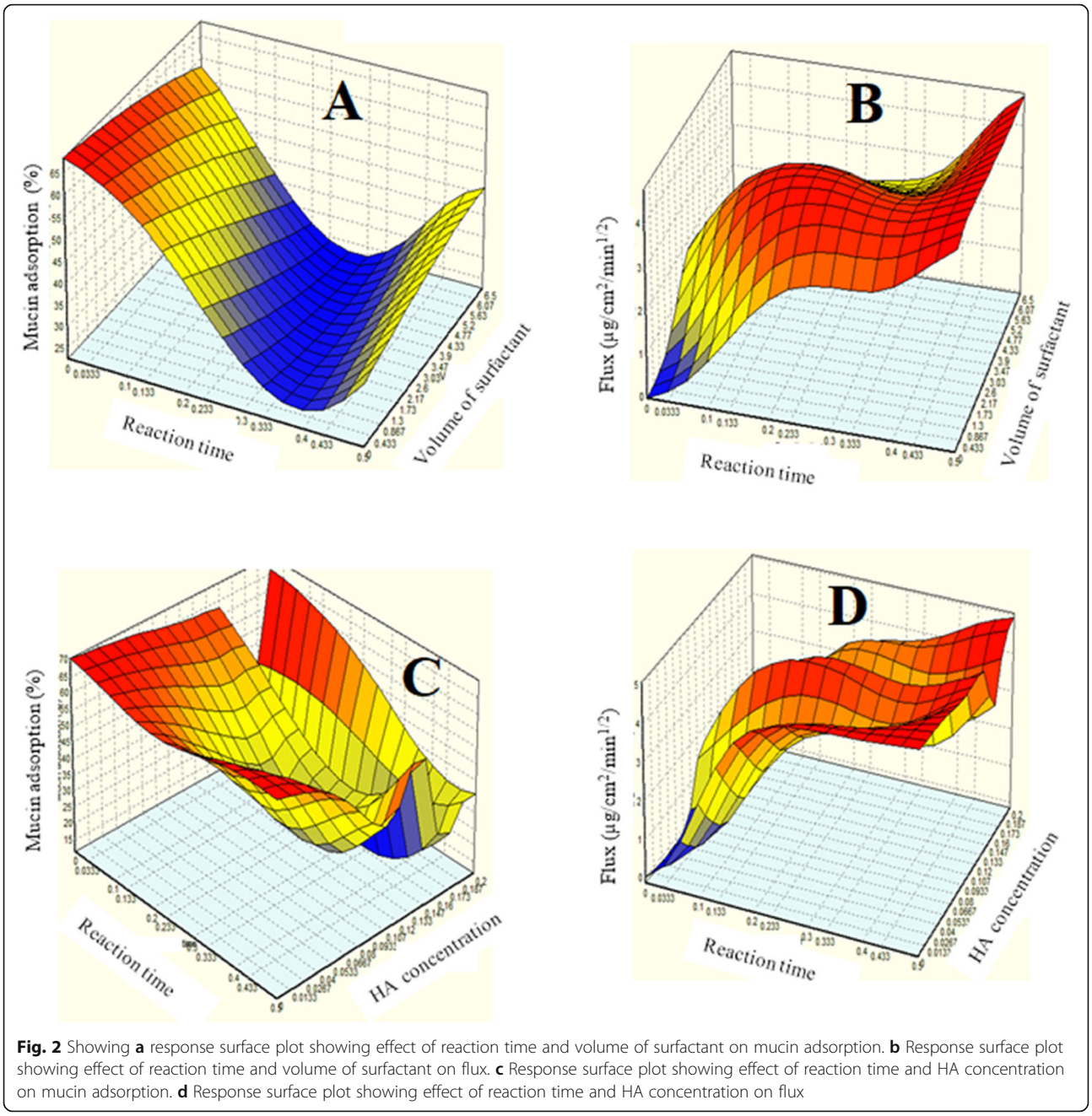

Fig. 2 Showing **a** response surface plot showing effect of reaction time and volume of surfactant on mucin adsorption. **b** Response surface plot showing effect of reaction time and volume of surfactant on flux. **c** Response surface plot showing effect of reaction time and HA concentration on mucin adsorption. **d** Response surface plot showing effect of reaction time and HA concentration on flux

Table 5 Optimized conditions for mucin adsorption

Variable	GA	RIO	PSO
HA concentration	0.13653	0.13654	0.13677
Volume of surfactant	5.89753	5.89791	5.90566
Reaction time	0.4999	0.5	0.4999
Maximum mucin adsorption (%)	70.84324	70.84329	70.84305

Table 6 Optimized conditions for flux

Variable	GA	RIO	PSO
HA concentration	0.15976	0.15977	0.15938
Volume of surfactant	6.49995	6.5	6.49875
Reaction time	0.49998	0.5	0.49976
Maximum flux	4.962	4.962	4.962

Table 7 Physicochemical characterization of the formulations

Formulation	Appearance	Viscosity (mPas at 40 rpm, 25 °C)	[b]Viscosity (mPas at 40 rpm, 25 °C)	pH at 25 °C	[b]pH at 25 °C	Osmolality (mOsm/kg)	[b]Osmolality (mOsm/kg)
[a]HAP organogel	Slight yellow gel	1476 ± 11.32	1430 ± 9.65	5.9 ± 0.07	6.1 ± 0.03	450.4 ± 1.01	455.5 ± 1.11
Optimized HAP organogel	Off white gel	1402 ± 9.43	1411 ± 11.32	4.9 ± 0.03	4.8 ± 0.07	399.1 ± 1.32	399.1 ± 1.06
Placebo gel (Nonoxynol-9 gel)	Transparent and colorless	2993 ± 4.99	3015 ± 1.03	4.2 ± 0.01	4.2 ± 0.01	91.1 ± 1.28	92.2 ± 1.46

[a]HAP organogel (see run 5 in Table 3)
[b]Results obtained after accelerated stability testing for 3 months

organogels exhibited shear thinning synonymous with non-Newtonian pseudoplastic effect where a decrease in viscosity is observed with an applied sheer on the formulation. This attribute is essential for drug release from the formulation. Application of sheer did not significantly affect the viscosity of the placebo gel nonoxynol 9. All formulations were seen to be sufficiently viscous and suitable for vaginal application. The organogels were stable over the 3-month accelerated stability testing period with no significant changes in viscosity, pH, and osmolality. The in vitro release study for the organogels showed a release rate of 3.894 $\mu g/cm^2/min^{1/2}$ for the HAP organogel, a higher value of 4.49 $\mu g/cm^2/min^{1/2}$ was obtained for the optimized

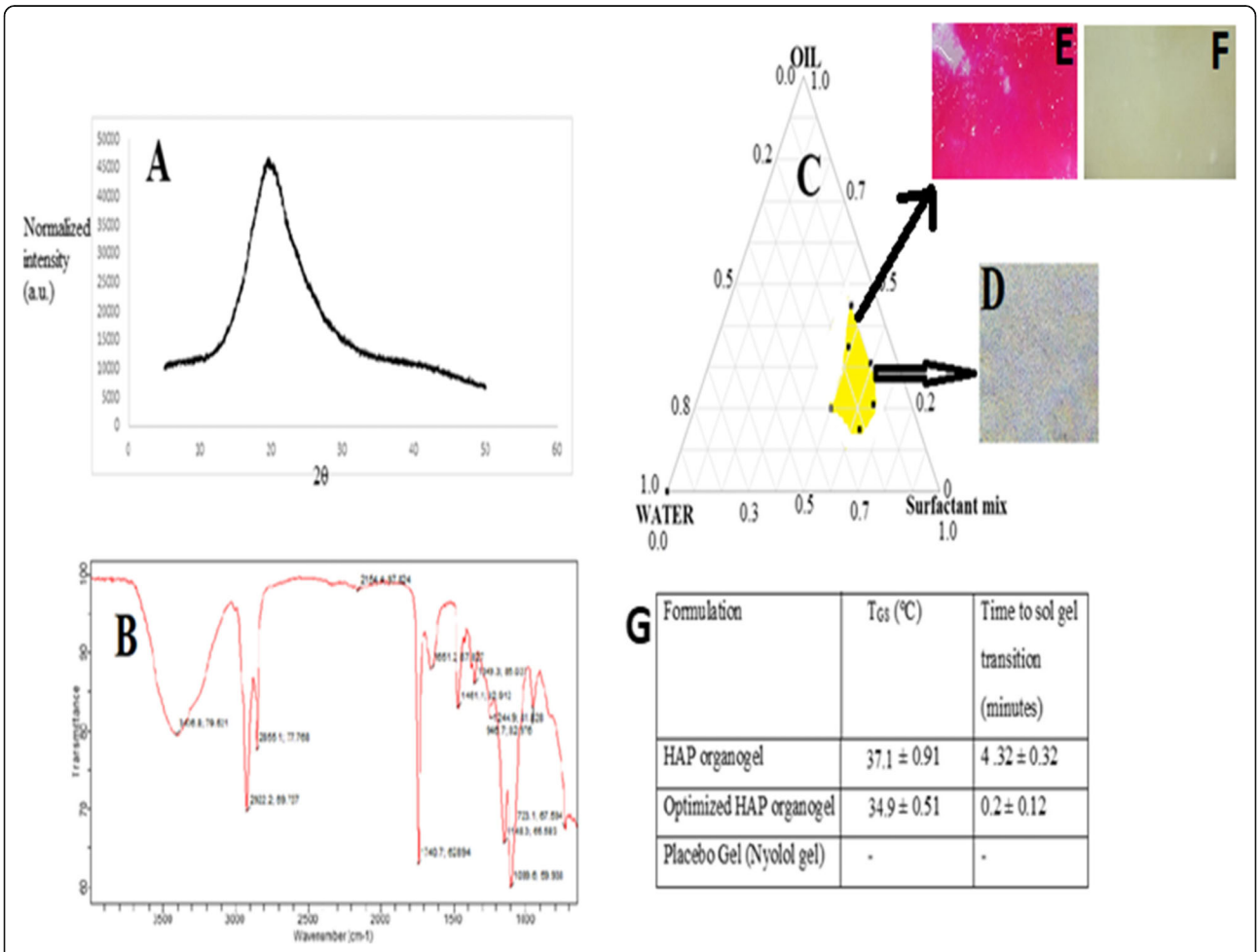

Fig. 3 Showing **a** X-ray diffractogram, **b** FTIR spectra, **c** pseudo ternary phase diagram, and **d** micrograph at × 80 magnification of the optimized hyaluronic acid-palm oil HAP-based organogel. **e** Optimized hyaluronic acid-palm oil HAP organogels prepared with aqueous rhodamine B solution. **f** Optimized hyaluronic acid-palm oil HAP organogel formulation. **g** Gel to sol transition temperature T_{GS} (°C) obtained using falling ball method of the optimized hyaluronic acid-palm oil HAP based

HAP formulation (Fig. 4a). Evaluation of the viability of *Lactobacillus crispatus* was carried out as shown in Fig. 5a where the organogels were seen to preserve the viability of *L. crispatus* when compared to control 48 h of incubation and proved non cytotoxic to HeLa cells over 14 days in vitro (Fig. 5a). HIV infectivity was seen to be decrease with increased concentration of the formulations as shown in Fig. 5c when the formulations were incubated with HIV-1 indicator TZM-bl cells at different concentrations.

Discussion

Maraviroc (MRV) a CCR5 antagonist has gained interest in its use for HIV prevention due to its activity as an entry inhibitor [6, 7, 22–24]. Due to the hydrophobic nature of MRV, its formulation as an organogel is designed to optimize drug release when compared to its release from a hydrophilic matrix like a hydrogel. With a log P of 2.4, pKa basic 7.3, during formulation MRV resides in the organic phase due to higher lipophilicity resulting in a stable interaction with HA in the fluid filled matrix

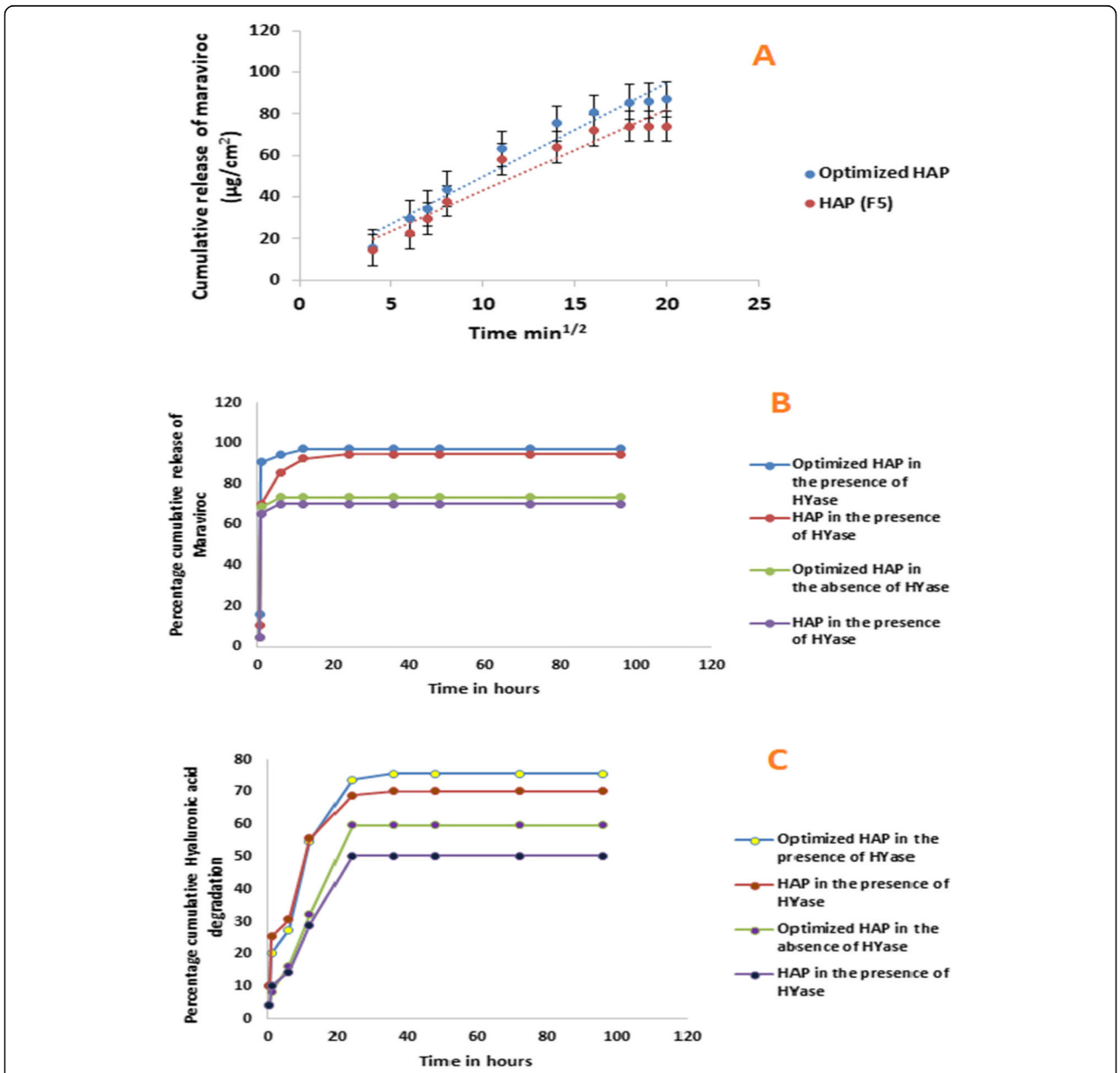

Fig. 4 a In vitro release of maraviroc from the optimized hyaluronic acid-palm oil (HAP)-based organogel and HAP organogel. **b** Percent cumulative release profile of Maraviroc in presence or absence of HYase and **c** percent cumulative release profile of hyaluronic acid degradation in presence or absence of HYase carried out at a pH of 7.1 for optimized HAP and HAP organogel formulation

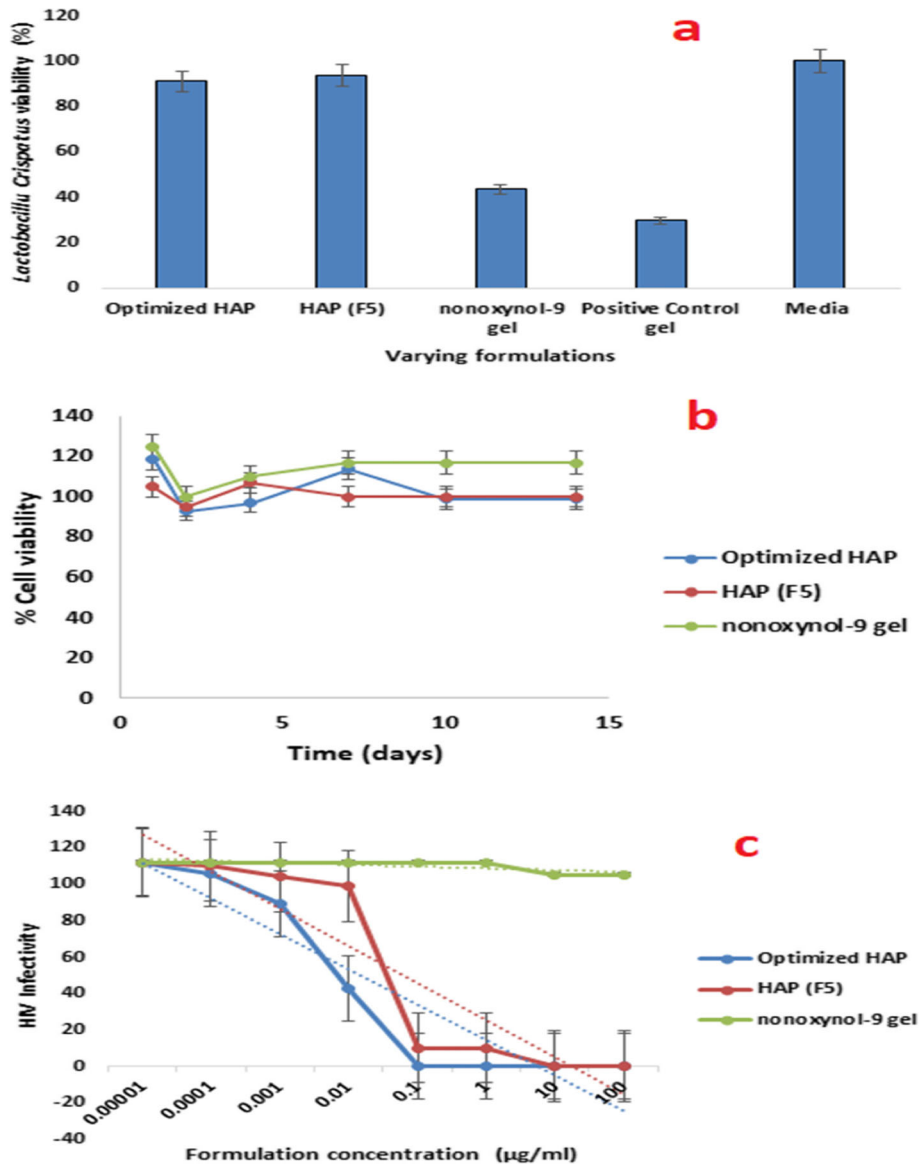

Fig. 5 **a** Lactobacillus viability assay after 48 h of incubation ($n = 3 \pm SD$). **b** HeLa cell cytotoxicity of optimized hyaluronic acid-palm oil (HAP)-based organogel and hyaluronic acid palm oil (HAP)-based organogel with HeLa cells over 14 days in vitro. Results are expressed as % cell viability compared to HeLa cells without any treatment ($n = 3 \pm SD$). **c** HIV infectivity dose-response curves for optimized HAP, HAP and nonoxynol gel incubated with HIV-1 indicator TZM-bl cells at different concentrations ($n = 5 \pm SD$)

hence optimizing product stability. The optimized HAP organogel was viscous with pH 4.5 and osmolality 399.1 mOsm/kg and pH 5.9 and osmolality 450.4 mOsm/kg for the un-optimized formulation. Vaginal formulations should have osmolality of less than 1000 mOsm/kg to prevent vaginal epithelial stripping [25], hence the formulated optimized organogels are postulated to be well tolerated when compared to CAPRISSA-004 tenofovir gel [22] and MTN-001 (nonoxynol 9) [26] gels which showed much higher osmolality. The optimized HAP organogel was thermosensitive, with optimal thermogelation point being 34.9 °C which was not too close to body temperature as recommended by CDER guidelines [27], compared to the un-optimized formulation which had 37.1 °C as its thermogelation point. This ensures enhanced stability in tropical countries where average temperatures as rated by ICH guidelines are higher than 30 °C [28, 29]. Sol to gel transition when exposed to body temperature was seen to be very short for the optimized formulation hence the optimized response to temperature exhibited by the optimized maraviroc organogel.

In this study, an optimized hyaluronic acid/palm oil (HAP)-based organogel as a vaginally administered pre-exposure prophylaxis agent was successfully developed

using artificial neural networks to model and optimize mucin absorption and flux. These responses were predicted using the MFFF and the MNFF neural networks. These parameters were necessary for the development of hyaluronidase trigger release of the incorporated antiretroviral agent maraviroc. The mucus secreted by the cervical epithelium provides a protection over the vaginal epithelium while encouraging sperm migration toward the cervix. Mucin adsorption was found to decrease with increase in reaction time as shown in Fig. 2a. This trend was observed both at low and high volumes of surfactants. Conversely, the volume of surfactant had very little influence on mucin adsorption at low levels of reaction time. However, at higher reaction times, the volume of surfactant was observed to positively influence mucin adsorption. Figure 2b shows that increasing the reaction time resulted in an increase in the level of flux. This trend was observed both at low and high volumes of surfactants. Similarly, increasing the volume of surfactant also resulted in an increase in the level of flux, although the effect was not as significant when compared to that of reaction time. Intermediate levels of HA concentration were necessary to achieve optimum levels of mucin adsorption and flux as shown in Fig. 2 c, d, hence postulated retention of the developed organogel on the vaginas' epithelial surface. Dezzutti et al. [23] demonstrated that ectocervical mucosal protection would require ten-fold more concentration of maraviroc to protect it from HIV infection; this is due primarily to the inability of the formulation to be retained on the mucosal surface. Ensign et al. [28] assumption on mucus penetrating of formulations for vaginal drug delivery to protect against herpes simplex virus is in consonance with our premise of optimization of mucin adsorption for the organogel formulation which would ultimately lead to increase drug release and retention at the vaginal mucosal surface [29–31].

The in vitro release study for the organogels showed a release rate of 3.894 μg/cm^2/min$^{1/2}$ for the HAP organogel, a higher value of 4.49 μg/cm^2/min$^{1/2}$ was obtained for the optimized HAP organogel formulation (Fig. 4a), hence showing that maraviroc was adequately released from the formulation; this result is similar to those obtained by Dezutti et al. [23], and that optimizing flux and mucin absorption translated in higher values of maraviroc release. In the presence of 1.08 U of hyaluronidase (an approximate concentration present in 3 ml of human semen ejaculate [10]), the cumulative release rate was subsequently evaluated with degradation analysis. The presence of hyaluronidase HYase initiates an enzymatic breakdown of free carboxylic acid groups of glucuronic acid present in hyaluronic acid which was utilized in the formulation. Both the optimized HAP organogel and HAP organogel showed a clear response to HYase via increase in the percentage release of maraviroc from the organogel in the presence of HYase (Fig. 4b, c). There was a 2.5-fold increase in the percentage of maraviroc release in the presence of HYase when compared with the percentage released in the absence of HYase. This efficient trigger mechanism for maraviroc release in response to the presence of hyaluronidase present in semen was highly efficient, when compared to the Agrahari et al. [10] whose trigger was just a component of the formulation and not the entire formulation. The optimized formulation facilitates drug release in the vaginal; the mucous layer did not affect the adsorption character of the organogel and by extension did not affect drug release.

The acidic environment of vagina is maintained by *Lactobacilli*, which lowers the risk of HIV infection by its natural defense mechanism [24, 26–28], hence any microbicide formulation will need to preserve the natural defense mechanism of the vagina by not disturbing the *Lactobacilli* viability. The organogels evaluated for safety via % *Lactobacilli crispatus* viability showed no significant change in the viability of *L. crispatus* when compared to media (Fig. 5a). There was a significant difference between the organogels formulated and controls utilized. In vitro cytotoxicity of the optimized HAP organogel was carried out to ensure that organogels did not cause any cytotoxicity to HeLa cells. All the formulations containing MRV concentration of 5 μg/ml did not have any significant toxicity observed compared to control cells or nonoxynol-9 gel (Fig. 5b). The concentration response model utilized in this study was developed to establish the ability of optimized HAP organogel for pre-exposure prophylactic management of HIV exposure. TZM-bl cells were treated with optimized HAP and F5 HAP organogel over a period of 12 h; the cells were washed, and media replaced followed by re-exposure to HIV cells after 24 h. Figure 5c shows that there was reduced infectivity with the cells treated with optimized HAP and F5 HAP organogel. The lower concentrations of the formulations (0.1 μg/ml of optimized HAP) were able to reduce HIV infectivity. The anti-HIV activity was due to the ability of the organogel to release maraviroc which was then transported and maintained in adequate concentrations inside the cells to prevent infectivity.

Conclusion

In this study, artificial neural networks were used to model and optimize mucin absorption and flux of palm oil/hyaluronic acid-based organogel for vaginal delivery of maraviroc. The optimized HAP organogel was viscous with pH 4.5 and osmolality 399.1 mOsm/kg and pH 5.9. The in vitro release study for the organogels showed a release rate of 3.894 μg/cm^2/min$^{1/2}$ for the HAP organogel, a higher value of 4.49 μg/cm^2/min$^{1/2}$ was obtained

for the optimized formulation. There was a 2.5-fold increase in the percentage of maraviroc release in the presence of hyaluronidase when compared with the percentage released in the absence of hyaluronidase, hence the effectiveness of the organogel to release maraviroc in the presence of hyaluronidase enzyme acting as a trigger. These data highlight the potential use of palm oil/hyaluronic acid-based organogel for vaginal delivery of anti-HIV microbicides. This can serve as a template for more studies on such formulations in the area of HIV microbicide development.

Abbreviations

AAD: Average absolute deviation; ANN: Artificial neural networks; BBP: Batch back propagation; CCD: Central composite design; CCR5: Chemokine receptor type 5; CD4 cell: Type of lymphocyte also called helper T cells; CDER: Center for Drug Evaluation and Research Food and Drug Administration; FTIR: Fourier-transform infrared spectroscopy; GA: Generic algorithm; HA: Hyaluronic acid; HAP: Hyaluronic acid/palm oil-based organogel containing maraviroc; HIV/AIDS: Human immunodeficiency virus/ Acquired immune deficiency syndrome; HYase: Hyaluronidase; IBP: Incremental back propagation; LM: Levenberg-Marquadt algorithm; MAD: Mean absolute deviation; MFFF: Multilayer full feed forward; MNFF: Multilayer normal feed forward; MRV: Maraviroc; MTT: 3-(4,5-Dimethylthiazol-2-yl)-2,5-diphenyltetrazolium bromide;; Optimized HAP: Optimized hyaluronic acid/ palm oil-based organogel containing maraviroc; PSO: Particle swarm optimization; QP: Quick propagation; RIO: Rotation inherit optimization; RMSE: Root mean square error; STIs: Sexually transmitted infections; TZM-bl cell: An adherent cell line that contains integrated reporter genes for firefly Luc and *E. coli* β-galactosidase under the control of an HIV-1 long terminal repeat; XRD: X-ray diffraction

Acknowledgments

Research reported in this publication was supported by the Fogarty International Center of the National Institutes of Health under Award Number D43TW010134. I also acknowledge Fisher Bioservices/NIH-ARP German town MD for the gift some reagents utilized in this study.

Authors' contributions

IMO carried out the experimental studies and drafted the manuscript. AAN carried out the artificial neural network modeling studies. AAS helped to design the studies, and IMO conceived of the study. ERF, AAO, and VV participated in its design and coordination, and helped to draft the manuscript. All authors have read and approved the final manuscript.

Funding

This work was financially supported by the Fogarty International Center of the National Institutes of Health under Award Number D43TW010134. The content is solely the responsibility of the authors and does not necessarily represent the official views of the National Institutes of Health.

Co-Funding Partners

Fogarty International Center (FIC)

NIH Common Fund, Office of Strategic Coordination, Office of the Director (OD/OSC/CF/NIH) Office of AIDS Research, Office of the Director (OAR/NIH) Office of Research on Women's Health, Office of the Director (ORWH/NIH) National Institute on Minority Health and Health Disparities (NIMHD/NIH) National Institute of Neurological Disorders and Stroke (NINDS/NIH). I declare that the funding body had no role in the design of the study, collection, analysis, and interpretation of data and in writing the manuscript.

Availability of data and materials

Data will not be shared because it contains unpublished data.

Ethics approval and consent to participate

Ethical approval was obtained from the Health Research and Ethics committee of the College of Medicine University of Lagos. CMUL/HREC Number: CMUL/HREC/02/18/332.

Consent for publication

Not applicable.

Competing interests

The authors declare that they have no competing interests.

Author details

[1]Department of Pharmaceutics and Pharmaceutical Technology, Faculty of Pharmacy, University of Lagos, PMB 12003, Surulere, Lagos, Nigeria. [2]Department of Pharmaceutics and Pharmaceutical Technology, Faculty of Pharmacy, University of Ilorin, Ilorin, Kwara, Nigeria. [3]Department of Chemical Engineering, Faculty of Engineering, University of Benin, Benin City, Nigeria. [4]Department of Electrical and Electronic Engineering, School of Engineering Manchester metropolitan University, Manchester M1 5GD, UK. [5]Department of Hematology and Blood Transfusion, College of Medicine, University of Lagos, Idi-Araba, Lagos, Nigeria.

Received: 23 September 2019 Accepted: 2 December 2019
Published online: 03 January 2020

References

1. Kelly CG, Shattock RJ (2011) Specific microbicides in the prevention of HIV infection. J Intern Med 270:509–519. https://doi.org/10.1111/j.1365-2796.2011.02454.x
2. Vandegraff N, Engelman A (2007) Molecular mechanisms of HIV integration and therapeutic intervention. Expert Rev Mol Med 9:1–19. https://doi.org/10.1017/S1462399407000257
3. Klasse PJ, Shattock RJ, Moore JP (2006) Which topical microbicides for blocking HIV-1 transmission will work in the real world? PLoS Med 3:e351. https://doi.org/10.1371/journal.pmed.0030351
4. Sagiri SS, Sethy J, Pal K, Banerjee I, Pramanik K, Maiti TK (2013) Encapsulation of vegetable organogels for controlled delivery applications. Des Monomers Polym 16(4):366–376. https://doi.org/10.1080/15685551.2012.747154
5. Meng J, Agrahari V, Ezoulin MJ, Purohit SS, Zhang T, Molteni A, Dim D, Oyler NA, Youan BC (2017) Spray-dried thiolated chitosan-coated sodium alginate multilayer microparticles for vaginal HIV microbicide delivery. AAPS J 19:692. https://doi.org/10.1208/s12248-016-0007-y
6. Brown KC, Patterson KB, Malone SA, Shaheen NJ, Prince HM, Dumond JB et al (2011) Single and multiple dose pharmacokinetics of maraviroc in saliva, semen, and rectal tissue of healthy HIV-negative men. J Infect Dis 203(10):1484–1490. https://doi.org/10.1093/infdis/jir059
7. Dumond JB, Patterson KB, Pecha AL, Werner RE, Andrews E, Damle B et al (2009) Maraviroc concentrates in the cervicovaginal fluid and vaginal tissue of HIV-negative women. J Acquir Immune Defic Syndr 51(5):546–553. https://doi.org/10.1097/QAI.0b013e3181ae69c5
8. Mizrahy S, Raz SR, Hasgaard M, Liu H, Soffer-Tsur N, Cohen K et al (2011) Hyaluronan-coated nanoparticles: the influence of the molecular weight on CD44-hyaluronan interactions and on the immune response. J Control Release 156(2):231–238. https://doi.org/10.1016/j.jconrel.2011.06.031
9. Schanté CE, Zubera G, Herlin C, Vandamme TF (2011) Chemical modifications of hyaluronic acid for the synthesis of derivatives for a broad range of biomedical applications. Carbohydr Polym 85:469–489. https://doi.org/10.1016/j.carbpol.2011.03.019
10. Agrahari V, Zhang C, Zhang T, Zhang T, Li W, Gounev TK, Oyler NA, Youan BC (2014) Hyaluronidase-sensitive nanoparticle templates for triggered release of HIV/AIDS microbicide *in vitro*. AAPS J 16:181. https://doi.org/10.1208/s12248-013-9546-7
11. Bajaj G, Kim MR, Mohammed SI, Yeo Y (2012) Hyaluronic acid-based hydrogel for regional delivery of paclitaxel to intraperitoneal tumors. J Control Release 158(3):386–392. https://doi.org/10.1016/j.jconrel.2011.12.001
12. Kalustian P (1985) Pharmaceutical and cosmetic uses of palm and lauric products. J Am Oil Chem Soc 62:431–433. https://doi.org/10.1007/BF02541417
13. Wong WS, Lee CS, Er HM, Lim WH (2017) Preparation and evaluation of palm oil-based polyesteramide solid dispersion for obtaining improved and targeted dissolution of mefenamic acid. J Pharm Innov 12:76–89. https://doi.org/10.1007/s12247-017-9271-3
14. Zainol S, Basri M, Basri HB, Shamsuddin AF, Abdul-Gani SS, Karjiban RA, Abdul-Malek E (2012) Formulation optimization of a palm-based nanoemulsion system containing levodopa. Int J Mol Sci 13:13049–13064. https://doi.org/10.3390/ijms131013049

15. Ramzi M, Kashaninejad M, Salehi F, Sadeghi AR, Ali SM (2015) Modeling of rheological behavior of honey using genetic algorithm–artificial neural network and adaptive neuro-fuzzy inference system. Food Biosci 9:60–67. https://doi.org/10.1016/j.fbio.2014.12.001
16. Amenaghawon NA, Amagbewan E (2017) Evaluating the effect of acid mixtures and solids loading on furfural production from sugarcane bagasse: optimization using response surface methodology and artificial neural network. Niger Res J Eng Environ Sci 2(2):578–587 http://www.rjees.com/abstract/evaluating-the-effect-of-acid-mixtures-and-solids-loading-on-furfural-production-from-sugarcane-bagasse-optimization-using-response-surface-methodology-and-artificial-neural-network
17. Ajala SO, Betiku E (2015) Yellow oleander seed oil extraction modeling and process parameters optimization: performance evaluation of artificial neural network and response surface methodology. J Food Process Preserv 39: 1466–1474. https://doi.org/10.1111/jfpp.12366
18. Betiku E, Odude VO, Ishola NB, Bamimore A, Osunleke AS, Okeleye AA (2016) Predictive capability evaluation of RSM, ANFIS and ANN: a case of reduction of high free fatty acid of palm kernel oil via esterification process. Energ Conver Manag 124:219–230. https://doi.org/10.1016/j.enconman.2016.07.030
19. Ilomuanya MO, Amenaghawon NA, Odimegwu J, Okubanjo OO, Aghaizu C, Adeyinka O, Akhimien T, Ajayi T (2018) Formulation and optimization of gentamicin hydrogel infused with *tetracarpidium conophorum* extract via central composite design for topical delivery. Turk J Pharm Sci 15(3):319–327. https://doi.org/10.4274/tjps.33042
20. Guan X, Yao H (2008) Optimization of viscozyme L-assisted extraction of oat bran protein using response surface methodology. Food Chem 106:345–351. https://doi.org/10.1016/j.foodchem.2007.05.041
21. Raymond EG, Lien CP, Luoto J (2004) Contraceptive effectiveness and safety of five nonoxynol-9 spermicides: a randomized trial. Obstet Gynecol 103(3): 430–439. https://doi.org/10.1097/01.AOG.0000113620.18395.0b
22. Dezzutti CS, Rohan LC, Wang L, Uranker K, Shetler C, Cost M, Lynam JD, Friend D (2012) Reformulated tenofovir gel for use as a dual compartment microbicide. J Antimicrob Chemother 67:2139–2142. https://doi.org/10.1093/jac/dks173
23. Dezzutti CS, Yandura S, Wang L, Moncla B, Teepl EA, Devlin B, Nuttal J, Brown ER, Rohan LC (2015) Pharmacodynamic activity of Dapivirine and Maraviroc single entity and combination topical gels for HIV-1 prevention. Pharm Res 32:3768. https://doi.org/10.1007/s11095-015-1738-7
24. Dezzutti CS, Russo J, Wang L, Abebe KZ, Li J et al (2014) Development of HIV-1 rectal-specific microbicides and colonic tissue evaluation. PLoS One 9(7):e102585. https://doi.org/10.1371/journal.pone.0102585
25. Date AA, Shibata A, Goede M, Sanford B, La Bruzzo K, Belshan M, Destache CJ (2012) Development and evaluation of a thermosensitive vaginal gel containing raltegravir+efavirenz loaded nanoparticles for HIV prophylaxis. Antivir Res 96(3):430–436. https://doi.org/10.1016/j.antiviral.2012.09.015
26. Van Damme L, Ramjee G, Alary M et al (2002) Effectiveness of COL-1492, a nonoxynol-9 vaginal gel, on HIV-1 transmission in female sex workers: a randomised controlled trial. Lancet 360:971–977. https://doi.org/10.1016/S0140-6736(02)11079-8
27. Guidance for Industry Vaginal Microbicides: Development for the Prevention of HIV Infection. Office of Communications, Division of Drug Information Center for Drug Evaluation and Research Food and Drug Administration (CDER 2014) http://www.fda.gov/Drugs/GuidanceComplianceRegulatoryInformation/Guidances/default.htm
28. Ensign LM, Tang BC, Wang YY, Tse TA, Hoen T, Cone R, Hanes J (2012) Mucus penetrating nanoparticles for vaginal drug delivery protect against herpes simplex virus. Sci Transl Med 4:138. https://doi.org/10.1126/scitranslmed.3003453
29. Lai SK, Hida K, Shukair S, Wang YY, Figueiredo A, Cone R et al (2009) Human immunodeficiency virus type 1 is trapped by acidic but not by neutralized human cervicovaginal mucus. J Virol 83(21):11196–11200. https://doi.org/10.1128/JVI.01899-08
30. Miller CJ, Li Q, Abel K et al (2005) Propagation and dissemination of infection after vaginal transmission of simian immunodeficiency virus. J Virol 79:9217–9227. https://doi.org/10.1128/JVI.79.14.9217-9227.2005
31. Haase AT (2011) Early events in sexual transmission of HIV and SIV and opportunities for interventions. Annu Rev Med 62:127–139. https://doi.org/10.1146/annurev-med-080709-124959

Publisher's Note